energies

Article

Energy and Economic Sustainability of a Small-Scale Hybrid Renewable Energy System Powered by Biogas, Solar Energy, and Wind

Rafał Figaj

AGH University of Krakow, Faculty of Energy and Fuels, Department of Sustainable Energy Development, al. A. Mickiewicza 30, 30-059 Krakow, Poland; figaj@agh.edu.pl

Abstract: Reduction or elimination of reliance on traditional fossil fuels and of the emission of greenhouse gases and pollutants into the environment are affecting energy technologies, systems, and applications. In this context, one potential approach to achieving sustainability, decarbonization, and ensuring the energy and economic viability of existing and future energy systems involves adopting one or more renewable sources. The presented paper concentrates on examining the performance of a small-scale hybrid renewable polygeneration system. This system utilizes biogas produced through anaerobic digestion, which is then supplied to an internal combustion engine, along with solar energy converted into electrical energy by photovoltaic modules and wind energy harnessed through a wind turbine. A small-scale user, represented by residential buildings and a zootechnical farm with heating, cooling, and electrical energy demands, serves as the case study. TRNSYS software is employed to design and model the system, considering realistic assumptions about technical aspects and user energy requirements. The investigation involves analyzing the system's operation, considering both energy and economic perspectives. The paper discusses the pros and cons of combining biogas, solar, and wind energy in the proposed hybrid system under the considered case study. Despite non-satisfactory economic profitability without incentives, the proposed system allows one to save significant amounts of primary energy and carbon dioxide equivalent emissions.

Keywords: biogas; solar energy; wind energy; polygeneration; energy analysis; economic analysis; residential; zootechnical; dynamic simulation

Citation: Figaj, R. Energy and Economic Sustainability of a Small-Scale Hybrid Renewable Energy System Powered by Biogas, Solar Energy, and Wind. *Energies* **2024**, *17*, 706. https://doi.org/10.3390/en17030706

Academic Editors: Sumit Roy, Shivaprasad Kumar Vijayalakshmi and Alessandro Giampieri

Received: 2 January 2024
Revised: 24 January 2024
Accepted: 30 January 2024
Published: 1 February 2024

1. Introduction

In the present-day energy sector, we observe a dynamic interplay of various forces. Among these forces are a surging energy demand, environmental concerns calling for enhanced energy efficiency and emissions reduction, and the increasing integration of renewable energy sources. Concurrently, sustainable development and emerging technological challenges exert their influence in shaping the new paradigms of the energy sector [1,2].

Conventional fossil fuels, once widely utilized without discrimination, have undergone a decline or even abandonment in various energy generation applications in favor of increasingly prevalent and reliable renewable energy sources [3]. However, this transition introduces fresh challenges in designing energy systems, primarily due to the inherent characteristics of renewables, such as their variability and intermittency [4]. These attributes render the technical adoption of renewables more intricate when compared to the programmable and manageable nature of conventional energy sources. Additionally, it is crucial to consider the relatively lower energy density, particularly noticeable in solar and wind energy applications [5].

Hybrid systems can provide a remedy for addressing challenges linked to individual renewable energy sources through the combination of two or more sources [6]. While hybrids are prevalent in medium- to large-scale applications, there is potential for small-scale hybrid renewable energy systems to revolutionize distributed generation [7]. In fact, such systems are common in microgrid applications [8], for which complex design and operation scheduling methodologies are applied [9,10]. Among the alternatives, biomass-based energy systems stand out due to their capability for both heat and electrical energy generation, coupled with ample source availability [11].

The existing scientific literature lacks comprehensive coverage of small-scale and micro-scale hybrid biomass systems (power lower than a few hundred kW), particularly those relying on combined heat and power units fueled by biogas, wind turbines, and photovoltaic modules. Typically, when dealing with the hybridization of biomass systems, only one additional energy source is considered. In a study [12], an integrated system featuring an organic rankine cycle (ORC) fueled by biomass and connected to a wind turbine was explored. The study evaluated component sizing and performance under various modes: full biomass, full wind, and two hybrid modes with different wind turbines and ORC units. The findings revealed that the ORC unit could be adjusted or partially operated during substantial wind output. Furthermore, hybrid systems reduced biomass consumption by up to 50% and diminished surplus electric energy by 40% to 70% compared to a fully biomass system.

The exploration of hybrid biomass-wind systems in microgrids is the subject of numerous studies. In one instance [13], a 100 kW wind turbine and a 150 kW biomass gasifier with energy storage were scrutinized for a village in India. The study employed real-time load data and HOMER software for energy-economic analysis. Results indicated that the wind-biomass gasifier system achieved a lower energy cost (USD 0.078) compared to a traditional wind-diesel engine setup (USD 0.165). Another study [14] delved into a hybrid system comprising a wind turbine, a biogas generator, and photovoltaic panels for a typical UK household. Using energy consumption data and thermoeconomic analysis with HOMER, the optimal configuration was determined to be a 1-kW wind turbine, a 1-kW biogas genset, and four 2.52 kWh battery units, resulting in the lowest levelized cost of energy (USD 0.588/kWh).

In a different hybridization endeavor [15], biomass-wind systems were enhanced with photovoltaic panels. A multi-objective optimization, considering economic and environmental factors, disclosed that a lower environmental impact correlated with higher system costs. Wind power was found to exert a significant positive impact due to its lower cost and environmental footprint compared to biomass and solar energy. A 50% reduction in emissions was achievable with a slight increase in investment costs. Examining a microgrid biomass combined heat and power (CHP) system, a study [16] has investigated the integration of small-scale wind turbines, biomass gasifiers, gas storage, photovoltaic modules, battery storage, thermal energy storage, and auxiliary boilers. Design and scheduling utilized an economic linear programming model. The most economically viable design encompassed a biomass CHP system combined with photovoltaic panels and batteries.

A hybrid microgrid system connected to the grid, incorporating wind, photovoltaics, and biomass, underwent evaluation in Pakistan [17] for both techno-economic feasibility and electricity generation potential. The Homer Pro software optimized the system for resilience and cost-effectiveness. The estimated cost of the 73.6 MW hybrid system was USD 180.2 million, with a levelized cost of energy amounting to USD 0.05744/kWh.

The exploration of small and micro-scale hybrid biomass-solar-wind systems, particularly their complex operation-energy-economic evaluation using dynamic simulations, remains an area of limited investigation. Hence, this paper introduces an analysis of the operation, energy, and economic performance of an innovative micro-scale polygeneration system. This system integrates anaerobic digestion based on zootechnical feces and corn silage, an internal combustion engine, an adsorption chiller, a wind turbine, and a photovoltaic field. To the best of the author's knowledge, in this paper, the proposed system and the considered case study are investigated for the first time in the literature by means of a dynamic modeling/simulation approach.

The investigation has been focused on the analysis of the system's dynamic operation and its energy and economic performance under real-world assumptions and user scenarios. The novelty of the paper lies in the investigated layout of the system, the small-scale case study, and the methodology adopted. As for the last one, in the current paper, it is the first time in scientific literature that a dynamic model for biogas generation and storage is coupled with a complex dynamic model of the installation, including the internal combustion engine, photovoltaic field, wind turbine, adsorption chiller, building, and a complex control strategy of the system. The modeling is based on the very realistic energy demand of the user; moreover, the system operation is simulated with a high time resolution in order to take into account the dynamic behavior of the system.

For this study, TRNSYS software v18.04 is employed, facilitating modeling and design as well as performance analysis through transient simulations. The paper delineates the system layout, operational strategy, and primary model assumptions. The case study involves a farm with five households situated in Polish seaside weather conditions (Gdańsk). Results are presented for a representative operation day and on a weekly and yearly basis. The paper concludes by summarizing the key findings of the research.

2. Materials and Methods

2.1. Layout and Operation of the System

In the proposed polygeneration setup (Figure 1), the generation of electrical energy is accomplished by employing a combined heat and power (CHP) unit utilizing an internal combustion engine, a wind turbine, and a photovoltaic field.

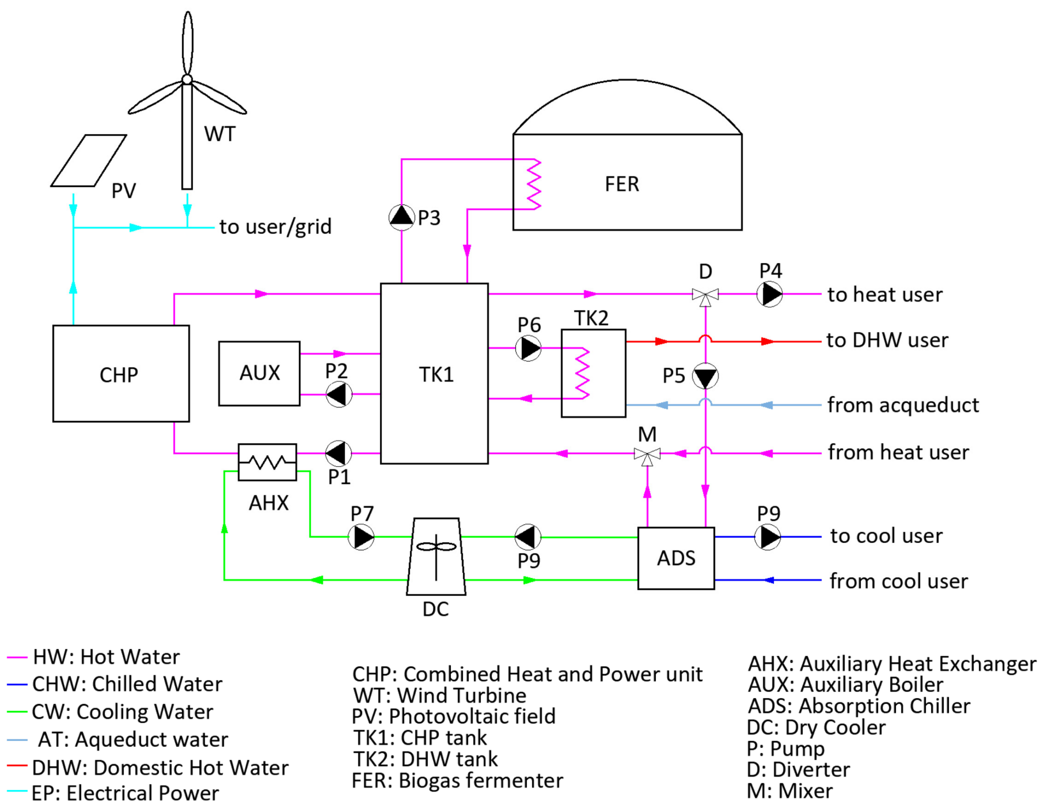

Figure 1. Layout of the system.

Concerning thermal energy, surplus thermal energy from the CHP is directed to the user heating system through a storage tank during the winter season. In the cooling season, the heat is harnessed to produce space cooling using an adsorption chiller. Furthermore, throughout the entire year, the generated thermal energy serves the dual purpose of meeting the demand for domestic hot water and heating the anaerobic digester to produce the necessary biogas to fuel the system.

The system under evaluation comprises multiple loops, delineated as follows:

- HW, hot water, serves as the working fluid for the thermal loops;
- CHW, chilled water, represents the water supplied by the chiller unit to the user for space cooling.
- CW, cooling water, is the water employed to dissipate the heat rejected by the chiller and/or produced in excess by the system;
- AT, aqueduct water, denotes water sourced from the mains and utilized in producing domestic hot water;
- DHW, domestic hot water, is the sanitary water consumed by the user;
- EP, electrical power, refers to the electrical output of the system and the power exchanged with the grid.

Furthermore, the system incorporates the following primary components:

- CHP, combined heat and power unit, an internal combustion engine fueled by biogas;
- WT, wind turbine, a horizontal-axis wind turbine;
- PV, photovoltaic field, a collection of monocrystalline photovoltaic modules;
- TK1, a stratified tank for storing heat produced by CHP, and an auxiliary heater;
- TK2, a tank dedicated to domestic hot water production;
- FER, a fermenter, an anaerobic digester for zootechnical feces and corn silage, equipped with biogas storage;
- AHX, auxiliary heat exchanger, employed to control the temperature at the CHP inlet;
- AUX, auxiliary boiler, a biogas boiler used to supplement the heat produced by CHP;
- ADS, adsorption chiller, responsible for producing space cooling;
- DC, dry cooler, used to dissipate heat from the system.

The system is also equipped with several pumps (P), a diverter (D), and a mixer (M) to regulate fluid flows within the system.

The control strategy of the proposed system is based on the following principles, listed in order to present the characteristics of operation:

- The CHP unit operates to maintain the temperature of TK1 between 62 and 65 °C, utilizing a proportional controller to set the load factor of CHP between 0.53 and 1.00.
- AUX is activated when the top temperature of TK1 drops to 59 °C and is turned off when a temperature of 63 °C is reached.
- The top temperature of TK2 is kept approximately 0.5 °C lower than the top temperature of TK1.
- FER temperature is maintained between 39 and 41 °C, utilizing a proportionally controlled diverter-mixer-bypass loop (not shown in Figure 1 for clarity) to manage the flow supplied to the internal heat exchanger of FER.
- The activation of AHX occurs when the inlet temperature of CHP exceeds 70 °C.
- ADS produces chilled water at 10 °C.
- The electrical power produced by CHP, WT, and PV is primarily supplied to the user, with excess power being sold to the grid.
- The grid is utilized to match the user's power demand in case the system's power output is insufficient.
- The electrical power consumed by CHP and FER auxiliary components accounts for 20% of the power output of CHP.
- The anaerobic digestion process is based on the use of cattle slurry and corn silage as substrates. The specific parameters considered for the substrates are as follows:
    - For cattle slurry: dry matter ratio of 0.1025; ratio of organic dry matter in dry matter of 0.8068; specific production of biogas per unit of substrate mass of 0.043 Nm^3/kg;

- For corn silage: dry matter ratio of 0.3267; ratio of organic dry matter in dry matter of 0.9357; specific production of biogas per unit of substrate mass of 0.240 Nm^3/kg.

The adopted values were sourced from technical data provided by a company producing biogas-powered cogeneration plants [18], and they align with literature data [19].

The summary of the operation assumption has been reported in Table 1.

Table 1. Operation assumptions for the proposed system.

Assumption	Value	Unit
ICE load factor range	0.53–1.00	-
TK1 temperature range for ICE	62–65	°C
TK1 temperature for AUX activation	59	°C
TK1 temperature for AUX deactivation	63	°C
TK1-TK2 temperature difference	0.5	°C
TK1 temperature range for ICE	39–41	°C
AHX activation temperature	70	°C
Set point temperature of ADS	10	°C
Auxiliary component power compared to CHP power	20	%
Cattle slurry dry matter ratio	0.1025	-
Cattle slurry ratio of organic dry matter to dry matter	0.8068	-
Cattle slurry-specific production of biogas per unit mass	0.043	Nm^3/kg
Corn silage dry matter ratio	0.3267	-
Corn silage ratio of organic dry matter to dry matter	0.9357	-
Corn silage-specific production of biogas per unit mass	0.240	Nm^3/kg

2.2. Model of the System

To simulate the hybrid system, it employed the widely used TRNSYS software [20], which is well-known for simulating various conventional and innovative energy systems [21–23]. The adopted methodology is summarized in Figure 2.

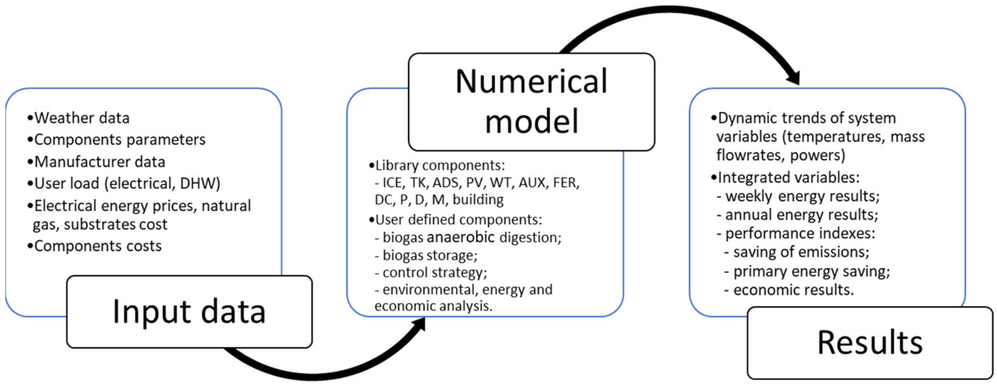

Figure 2. Methodology adopted for system modeling and analysis.

The starting point obviously was the developed concept of the system, for which input data has been used, such as weather data, technical parameters, load profiles, and cost parameters. After that, the model was developed using available resources in TRNSYS software, including ready models of the components and the possibility to implement own calculations/models. At the end, the results of the simulations were analyzed in the form of dynamic trends of system variables and summary data achieved by means of the integration of key variables (thermal and electrical powers).

In particular, the modeling of the system included the utilization of both pre-existing library components (e.g., CHP, WT, PV, pumps, mixers, diverters, valves, controllers, tanks, boilers, etc.) and the creation of user-defined components tailored to the system's design requirements. It is crucial to emphasize that the library components in the software have undergone experimental validation and are grounded in manufacturer data, ensuring the reliability of simulation outcomes.

In this section, the energy and economic model employed to assess the overall system performance is presented, omitting the details of other component models for brevity, which can be found in the TRNSYS software reference. Notably, the wind turbine model was developed based on manufacturer data [24], and the same applies to the adsorption chiller [25] and the ICE unit [26].

The model of the fermenter relied on a variable-volume tank model available in TRNSYS for the fluid part. The calculation of the cumulative biogas production for each feeding supply of substrate over time employed a modified version of the Gompertz function [19], while a simple model based on the balance of volumes was used to simulate the biogas storage operation.

The overall model was based on the realistic energy demand of the user, based on electrical, thermal (heating and cooling), and domestic hot water demand dynamic profiles with a time step of 5 min. Moreover, the system operation was simulated with a time step of 2.5 min in order to take into account the dynamic behavior of the system and achieve convergency in the calculations. The economic model was based on simple but very reliable assumptions, which were connected to the estimation of system investment costs and operation expenditures. Please note that the cost of the system components as well as the energy tariffs (biomass and electrical energy) were based on real market conditions, reflecting real-world conditions.

The TRNSYS components (types) utilized in developing the system model are listed in Table 2.

Table 2. TRNSYS built-in components used in the development of the system model.

Component	TRNSYS Type	Component	TRNSYS Type
ICE	907	DC	511
WT	90	P	3d
PV	562	M	11
TK1	534	D	11
TK2	340	buildings	56
FER (fluid model)	39	on/off controller with hysteresis	2
AHX	92	data plotters	65c
AUX	700	data integrator	24
ADS	909	data reader	9e
		weather data processor	109, 15

2.2.1. Energy and Economic Model of the System

To assess the overall energy and economic performance of the proposed system (PS), a comparison was made against two reference systems (RS), grounded on the premise that both the PS and RS should deliver an equivalent amount of final energy to the user, encompassing heating, domestic hot water, cooling, and electrical energy.

Specifically, two reference systems were outlined as follows:

- The NG system, relying on a natural gas boiler for heating, an electric chiller for cooling, and the electric grid for supplying electrical energy;
- The BIO system, utilizing a wood chip boiler for heating and the same two components as the NG system for cooling and electrical energy.

To compute the primary energy consumption/savings and economic performance of PS versus RS systems, a boiler system efficiency of 0.90, an electric chiller coefficient of performance (COP) of 3.0, and a national electric grid efficiency of 0.33 [27] were assumed.

The calculation of the generation of emissions was performed on the basis of equivalent CO_2 emissions for electrical energy supplied by the national electrical grid and natural gas consumption. The emission factors for electrical energy and natural gas were 0.65556 and

0.19973 $kgCO_{2,eq}$/kWh, respectively [28,29]. The generation of net emissions concerning the combustion of biogas in PS and wood chips in RS in the BIO scenario was neglected, since it has been assumed that the combustion products of both fuels will be fixed again in the organic matter.

The economic performance of the PS was evaluated by considering both the investment costs of the PS and the operating costs of both the PS and RS. Specifically, capital cost data from the market were employed to determine the PS component costs, following the procedure detailed in Refs. [30,31]. The cost of the ICE system with biogas production was estimated at 10.0 kEUR/kW on the basis of market data, while the photovoltaic field was valued at 370 EUR/m^2 [32]. Additionally, the cost of the adsorption chiller was set at 600 EUR/kW [33]. The wind turbine cost was determined based on a cost function available in Reference [34]. The overall system cost encompassed expenses related to balance-of-plant components, assumed to be 20% of the total cost of the main components of the system (CHP-FER, WT, PV, and ADS).

Concerning operating costs, a natural gas price of 0.07347 EUR/kWh was considered for the NG RS system [35]. For the biomass price in RS, two scenarios were considered: (1) free wood chips sourced from local residual biomass, and (2) a market price for biomass fuel at 0.06 EUR/kg, characterized by a lower heating value of 3.7 kWh/kg [34]. The price of corn silage used in the PS was set at 50 EUR/t, while the cost of cattle slurry was negligible, assuming its availability from the zootechnical farm.

Additionally, a constant tariff of 0.3080 EUR/kWh was applied for electrical consumption from the grid [36], while a time-dependent tariff [37] was implemented for the sale of excess electrical energy.

The economic parameters used in the simulation are summarized in Table 3.

Table 3. Environmental, energy, and cost parameters used in the model.

Parameter	Value	Unit
RS boiler efficiency	0.9	-
RS electric chiller COP	3.0	-
National electric grid efficiency	0.33	-
emission factor for electrical energy	0.65556	$kgCO_{2,eq}$/kWh
emission factor for natural gas	0.19973	$kgCO_{2,eq}$/kWh
ICE system cost with biogas production	10.0	kEUR/kW
PV field-specific cost	370	EUR/m^2
ADS-specific cost	600	EUR/kW
Natural gas price	0.07347	EUR/kWh
Market price for wood chip biomass	0.06	EUR/kg
Wood chip lower heating value	3.7	kWh/kg
Corn silage price	50	EUR/t
Purchase electrical energy tariff	0.3080	EUR/kWh
Sell electrical energy tariff	time variable	EUR/kWh

Considering the two wood chip pricing scenarios and the two reference systems, the economic viability of the proposed system was assessed in terms of savings and the simple payback (SPB) index across three scenarios:

- NG: utilization of natural gas in RS;
- BIO1: utilization of free wood chips in RS;
- BIO2: utilization of market-priced wood chips in RS.

2.2.2. Case Study

To evaluate system performance, a representative zootechnical farm was chosen as the case study, encompassing five households featuring a single-floor sloped roof structure with an attic in addition to a farming hall. Each household covered a floor area of 100 m^2, while the farm hall spanned 500 m^2. The house had a floor height of 2.7 m, while the halls ranged from 3.5 to 5.5 m in height. Climatic conditions were simulated using Meteonorm weather data for Gdansk, located in northern Poland. The building orientation, structure, and layout for this case study are depicted in Figure 3. Detailed thermal parameters for the buildings are available in Ref. [34].

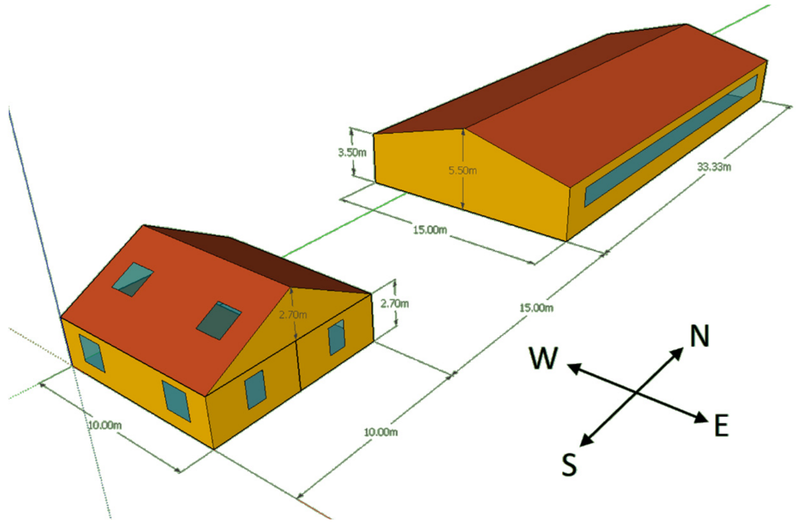

Figure 3. Case study buildings.

The heating and cooling system maintained indoor air temperatures of 20 °C during winter and 26 °C during summer within the households, operating on a 24/24-h schedule. For the hall, the air temperature was set to 10 °C in winter and 28 °C in summer. The building model was developed using the SketchUp tool, v17.2.2555 complemented by the TRNSYS3d v1.0.7.1 plug-in [20]. Furthermore, the thermal behavior of the considered buildings was simulated, taking into account thermal loads from equipment, lighting, fresh air infiltration, and other factors. Specifically, the infiltration rate for fresh air was set at 3 Vol/h for the hall and 0.3 Vol/h for the households. The heating and cooling loads of buildings have been presented in Figures 4 and 5.

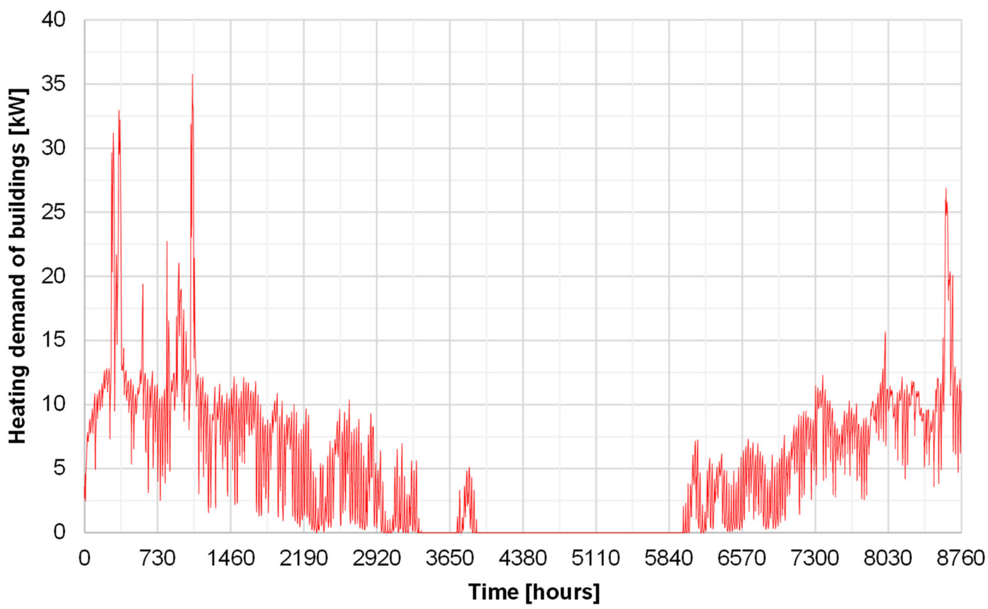

Figure 4. Heating demand of the buildings.

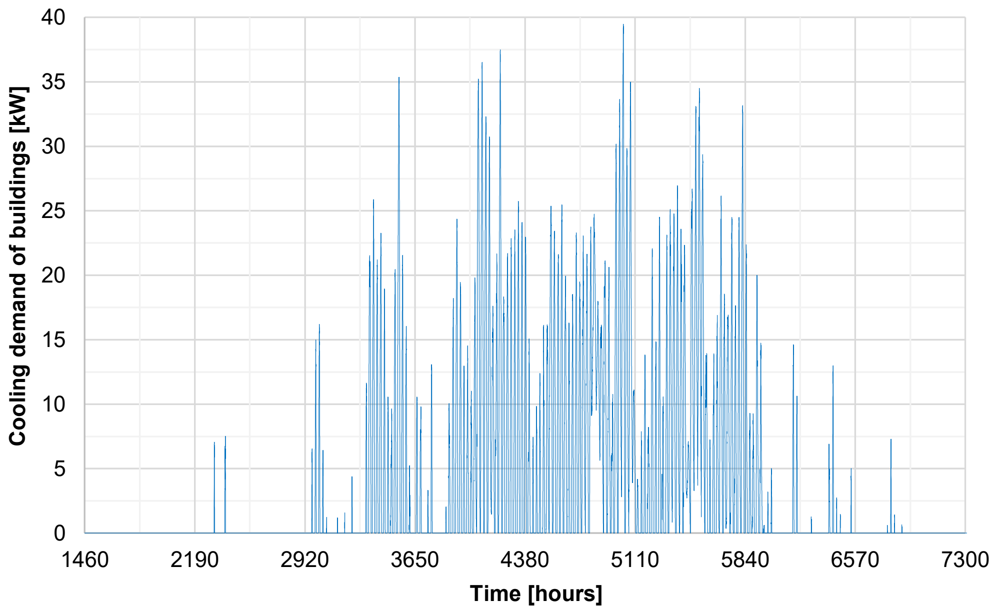

Figure 5. Cooling demand of the buildings.

To simulate domestic hot water (DHW) usage, demand profiles from relevant literature representing the user type examined in this paper were utilized [38]. Specifically, three average user profiles, measured at a 5-min sampling time, formed the basis for developing the user DHW demand. These profiles were normalized to establish the demand for each building, accounting for water usage equivalent to that of four people with a specific consumption of 60 kg/day/person at a temperature of 45 °C. The resulting DHW demand is depicted in Figure 6.

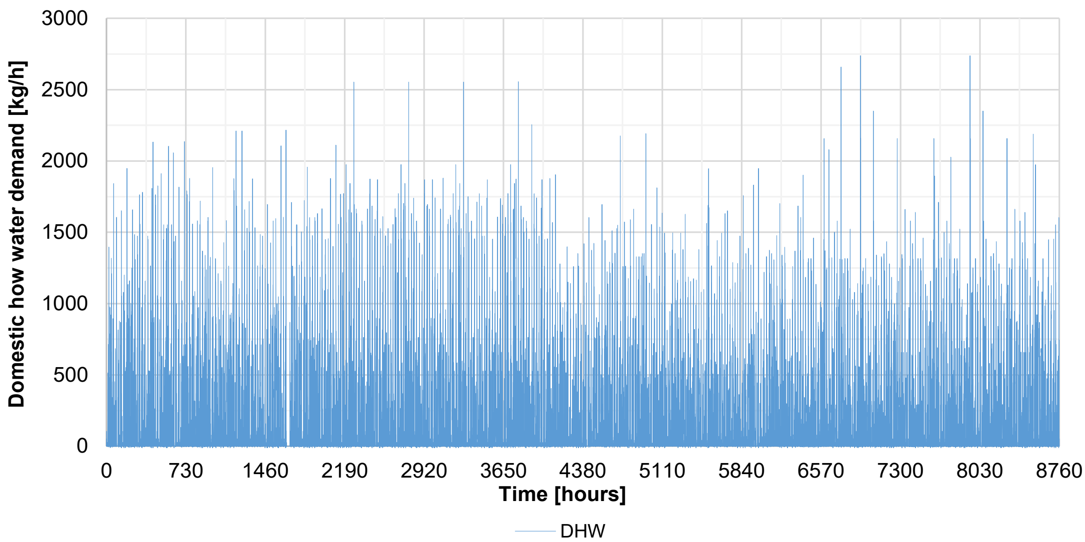

Figure 6. Domestic hot water demand of the user.

To model the electrical energy demand, standard profiles from the electricity company for users analogous to the one under investigation [39] were adopted. These profiles are based on typical hourly energy demands for various seasons and day types (workday, Saturday, Sunday/holiday). The annual electrical energy consumption was set at 100 MWh for the hall, aligning with common energy demand levels for this utility category [40]. For the households, the electrical energy consumption was set at 3 MWh.

Finally, Table 4 provides an overview of the essential system parameters, carefully chosen to ensure both efficient system design and operation concerning energy flows and thermodynamic characteristics.

Table 4. Main parameters of the main system components.

Parameter	Value	Unit	Parameter	Value	Unit
CHP power	15	kW	FER digestate volume	200	m^3
WT power	5	kW	FER biogas volume	600	m^3
PV power	5	kW	FER set point temperature range	39–41	°C
TK1 volume	20	m^3	AUX thermal power	75	kW
TK1 set point temperature range	62–65	°C	ADS cooling power	60	kW
TK2 volume	5	m^3	ADS chilled water set point	10	°C
TK2 threshold	0.5	°C			

The proposed system is fully scalable since the size/capacity of the components, such as the internal combustion engine, photovoltaic field, wind, adsorption chiller, thermal storage, and peak boiler, can be adapted to the available devices on the market and to the energy needs of the user. The adopted configuration of the system was assumed in order to match the user energy demand and achieve robust operation of the system. In particular, a simple iterative approach based on the energy levels produced by the components has been adopted in order to match the demand of the user.

3. Results

The developed dynamic simulation model offers insights into varying trends, encompassing temperature and power, along with integrated variables. However, to maintain brevity, this paper concentrates on crucial findings by highlighting the characteristics of operation for a representative day, weekly energy flows, and presenting annual energy and economic outcomes. All outcomes stem from simulations conducted with a time step of 5 min over the course of an entire year (0–8760 h).

In order to present a typical operation day for the proposed system, 16 February (from 1104 to 1128 h) has been selected. From the point of view of thermal energy usage, the behavior of the system in winter is essentially similar to the one achieved during the summer period, since the thermally driven chiller requires heat instead of the heating system of the user. The electrical power of PV and WT may achieve different trends in summer compared to winter; nevertheless, the effect on the system's operation is limited to the power supplied to or by the grid. Thus, for reasons of brevity, the operation for a representative winter day has been shown. In Figure 7, the main thermal power flows have been presented during the selected period. The thermal power produced by ICE stays at its nominal value during the first hours of the day due to the relatively high thermal demand for heating and the almost constant heating requirement of FERM. Apart from some peaks, DHW demand in such a period is significantly lower than the other ones; thus, its effect on the operation regime of ICE is marginal. In fact, only when the heating demand of buildings drops in the central hours of the selected day does the cogenerated ICE thermal power decrease. This is due to a lower thermal output needed to keep TK at the required temperature level (62–65 °C). It is interesting to note that the thermal power recovered from ICE in the last hours of the selected day does not increase as a function of the rising thermal demand for heating, since the thermal storage capacity of TK is adequate to face small variations of the thermal demand. However, this is also due to the decrease in FERM thermal demand during the same period. Due to the adoption of TK1 and TK2, it is also possible to cushion the effect of the rapid increase in DHW thermal demand during peaks on the operation of ICE. Indeed, the peaks of DHW demand determine only relatively small variations of the ICE operation point.

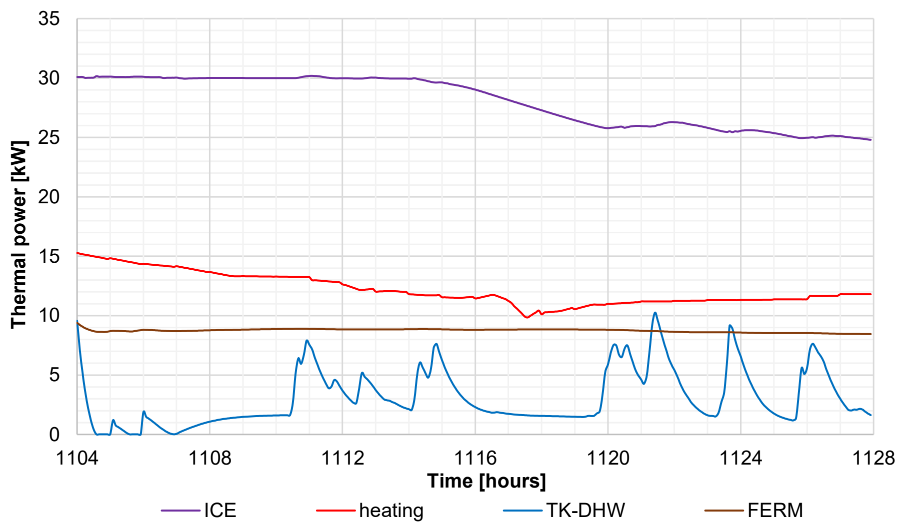

Figure 7. Thermal powers of the system—16 February.

In Figure 8, the main electrical powers have been presented. As expected, the ICE electrical power output presents the same trend as the thermal one. Obviously, the electrical power is hardly limited by the capacity of the device, as shown in the first hours of the selected day, while the thermal power produced (see Figure 7) is slightly affected by the variation of the returning temperature from TK1 to ICE. Peaks of DHW demand during the operation of ICE at nominal conditions determine a small increase in the thermal output of the device.

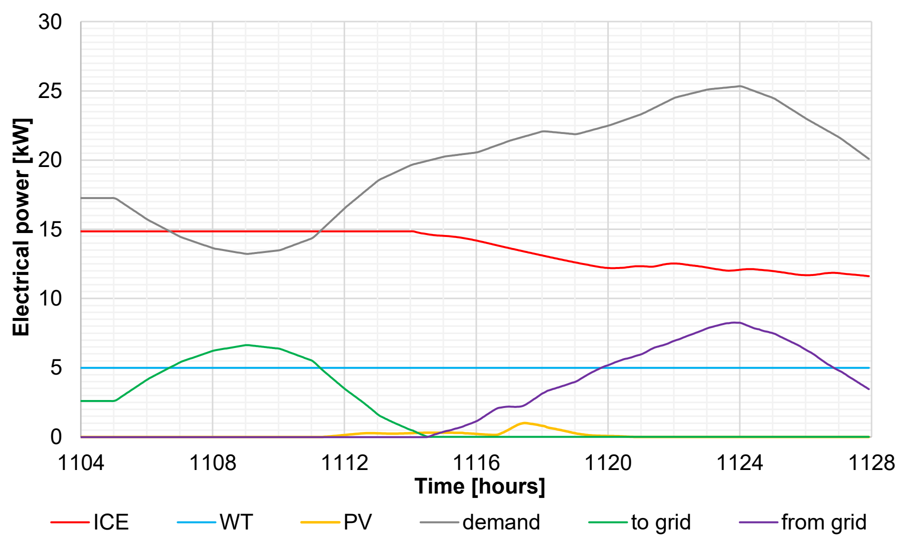

Figure 8. Electrical powers of the system—16 February.

During the selected day, the electrical demand of the user and system is lower at the beginning of the day, which allows one to produce electrical energy in excess, which is sold to the grid. This is also favored by the operation at the nominal condition of WT due to the high availability of wind. On the other hand, the power produced by the PV system is relatively low, as the solar radiation is scarce during the selected day. The power production from ICE, WT, and PVF amounted to 72.7, 26.7, and 0.6% of the total electrical energy produced from renewables.

The production of electrical power from renewables in the system allows the user to match the demand without the contribution of the grid for the first part of the day. As regards the excess energy, it accounted for 9.7% of the total energy produced, while the energy required from the grid accounted for 13.8% of the total demand during the considered day.

Figure 9 illustrates the weekly thermal energy flows. In the presented case study, the heat generated by the ICE was lower during the mid-seasons compared to winter and summer due to reduced space conditioning demand in those periods. For instance, in the 39th week, the thermal output was 52.7% lower than the peak achieved in the 33rd week. During winter, the CHP unit achieved approximately the same thermal energy output as in the summer. Despite the fact that there is significant demand for heating FERM and production of DHW in midseason, a part of the system's thermal energy must be dissipated by AHX in order to keep the return temperature to the heat recovery from ICE below 70 °C. Analyzing the activation of auxiliary heating by TK through AUX, it is evident that this occurs when the CHP system fails to produce a sufficient amount of thermal energy compared to the demand for space conditioning. However, TK1 maintains a consistent temperature range with a relatively small reliance on AUX, which diminishes during the mid-season period.

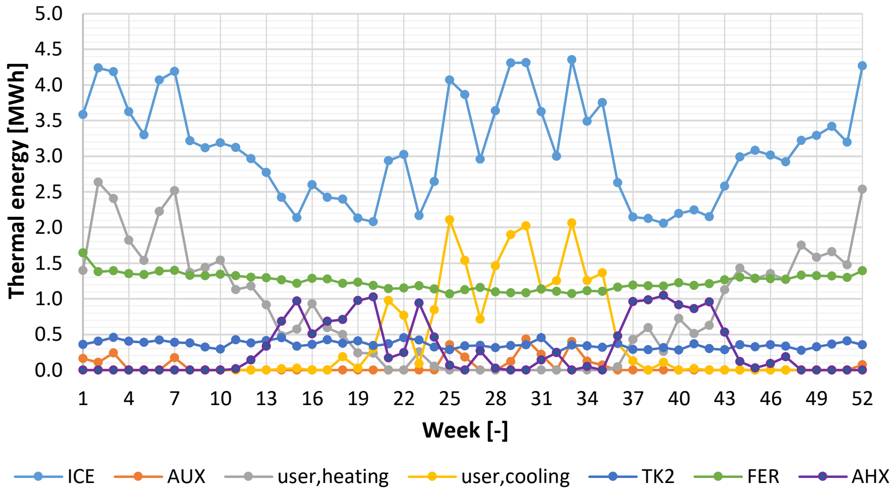

Figure 9. Weekly thermal energies.

TK1 provides more heat to FER during the winter weeks, as the lower air temperatures in this period necessitate increased heating compared to the summer months. On an annual basis, the heat supplied to FER varies by 35.1% relative to the maximum value observed in the first week of the year.

Figure 10 illustrates the weekly electrical energies of the system. The trend in electrical energy produced by ICE corresponds to the thermal energy generated by the same component. This correlation is due to the direct impact of the heat demanded by the system on ICE electrical power, following a thermal load strategy. Notably, the variation of energy output on a mean basis between winter and summer weeks is not significant, with energy production during the summer months differing by approximately −15.0% compared to winter. Consequently, the ICE operates at a lower load only during the mid-seasons.

The wind turbine's energy yield indicates that wind sources' availability in the selected locality is lower during summer compared to winter, conveniently aligning with reduced excess electrical energy production. Indeed, during the same summer period, user electrical demand also decreases. However, for PV, production levels increase in the summer weeks, contributing in part to the supply of electrical energy to the grid. The highest weekly energy production values are 4.35 MWh for ICE, 0.79 MWh for WT, and 0.25 MWh for PV. The electrical energy taken from the grid significantly exceeds the excess energy supplied to it. This is primarily due to the relatively high user electrical energy demand that limits surplus energy production.

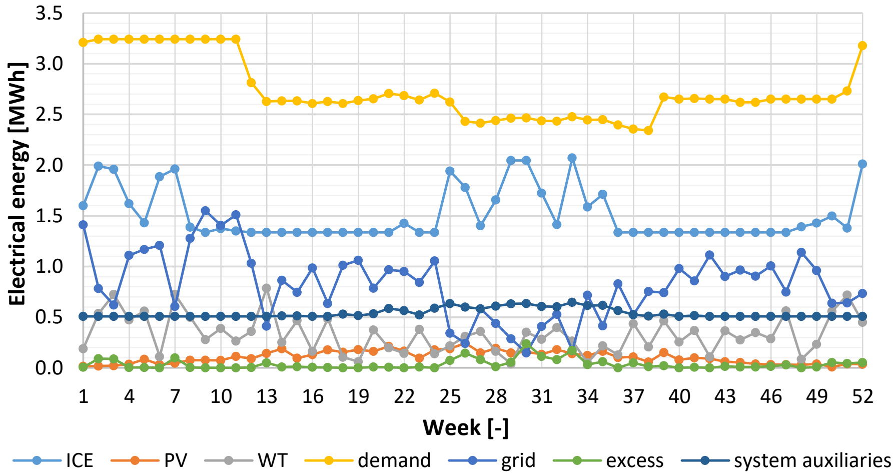

Figure 10. Weekly electrical energies.

Table 5 provides details on the thermal and electrical energies generated by the main components of the system. Particularly, ICE contributes significantly more to thermal energy production compared to the auxiliary heating system AUX. In fact, only 1.6% of the system's thermal energy output is generated by AUX. This is attributed to the infrequent activation of AUX for heating TK1, while ICE operates at almost full load throughout the space conditioning period. The heat produced by the system is used at 27.8% for space heating, 11.5% for DHW production, 20.6% for cooling production, and 40.2% for FER heating.

Table 5. Yearly thermal and electrical energies of the main system components.

Thermal Energy		Electrical Energy	
Component	**Value [MWh]**	**Component**	**Value [MWh]**
ICE	161.86	ICE	78.68
AUX	2.66	WT	17.30
user, heating	44.84	PV	5.49
user, cooling	20.66	user	114.41
user, DHW	18.57	auxiliaries	28.13
ADS, generator	33.20	demand	142.54
ADS, evaporator	20.66	to grid	1.82
FER	64.83	from grid	42.88
AHX	15.80		

In terms of electrical energy production, ICE, WT, and PVF contribute to 77.5%, 17.1%, and 5.4% of the total annual yield, respectively. Notably, ICE plays the most significant role in energy production, followed by the other components. Furthermore, the produced electrical energy meets 69.9% of the user demand, while the excess electrical energy accounts for only 1.8% of the total produced.

Table 6 contains the energy, environmental, and economic indicators obtained in the analysis. ICE performance is restricted by its relatively small size, resulting in a total efficiency of just over 80%. This result is characteristic of internal combustion engines with relatively small power, and it is consistent with the manufacturer's data. The energy production levels of the wind turbine and the equivalent number of operation hours, which are more than 3000 h, indicate that the chosen location is suitable for the installation of micro-scale wind turbines, especially in terms of energy yield. Concerning the photovoltaic system, the modules exhibited an efficiency below the reference value of 21% due to their operation beyond the reference temperature.

Table 6. Energy, environmental, and economic parameters of the system.

Result	Value	Unit	Result	Value	Unit
electrical efficiency, ICE	0.267	-	primary energy consumption, NG, RS	442.0	MWh
thermal efficiency, ICE	0.550		primary energy consumption, BIO, RS	367.6	MWh
electrical efficiency, PV	0.192	-	primary energy saving ratio, NG, PS	0.718	-
equivalent number of operation hours, WT	3460.6	h	primary energy saving ratio, BIO, PS	0.661	-
Coefficient of performance, ADS	0.622	-	savings, NG	12.14	kEUR/year
CO_2 equivalent emission, NG, RS	94.38	$tCO_{2,eq}$	savings, BIO1	6.67	kEUR/year
CO_2 equivalent emission, BIO, RS	79.52	$tCO_{2,eq}$	savings, BIO2	7.88	kEUR/year
CO_2 equivalent emission reduction, NG, PS	67.46	$tCO_{2,eq}$	system cost	235.13	kEUR
CO_2 equivalent emission reduction, BIO, PS	52.60	$tCO_{2,eq}$	SPB, NG	19.37	years
CO_2 equivalent emission reduction ratio, NG, PS	0.715	-	SPB, BIO1	29.84	years
CO_2 equivalent emission reduction ratio, BIO, PS	0.661	-	SPB, BIO2	35.24	years

The annual operation of the adsorption chiller achieves a COP of 0.661, considered satisfactory when taking into account the performance of the adsorption-based thermally driven chiller and the adopted control strategy regarding temperature levels inside TK1. The achieved value is below the maximum value of about 0.7 due to a different temperature regime of operation compared to the nominal conditions (lower chilled water temperature and variable cooling temperature).

The proposed system is able to achieve a relatively high reduction in CO_2 equivalent emissions compared to both scenarios for the reference system. For both cases, the reduction is above 65%. Is it interesting to note that, despite a higher demand for heat with respect to the one for electricity, the adoption of natural gas instead of biomass in the reference system does not produce a significant variation in the savings in emissions. In fact, as shown in Table 6, the difference in CO_2 equivalent emissions for NG and BIO is relatively small. This occurs because the major source of emission of CO_2 equivalent is due to the electrical load of the user. Similar results are achieved for the primary energy saving ratio, due to the previously mentioned latter reason. Indeed, the primary energy consumptions of RS in NG scenario compared to BIO one is only 16.8% higher.

The economic analysis revealed some differences in potential savings with the proposed system compared to the considered reference cases, primarily due to the lower cost of biomass per unit of energy compared to natural gas. Considering the economic parameters that have been chosen, SPB ranges from about 19 to 35 years for the scenarios examined. This highlights that beyond the relatively high system-specific costs, the economic viability of the hybrid setup is affected by the choice of fuel in the reference system. However, the proposed system achieves an unsatisfactory economic performance for the considered case study even under the NG scenario. One possible way to improve economic performance could be through the adoption of capital and energy production-based incentive policies. Under the actual cost of the system components, it is hardly advisable to adopt the proposed system without incentive policies.

4. Conclusions

The analysis undertaken demonstrates the technical and energy feasibility of the proposed system, which is capable of satisfying a significant portion of the user's energy needs while reducing dependence on the auxiliary boiler and electrical grid. Under the considered case study scenario, the performance of the system is also satisfactory from the primary energy and emissions-saving point of view. In fact, the proposed system allows one to reduce more than 65% of both primary energy consumption and CO_2 equivalent emissions.

Despite the relatively high initial investment cost associated with the proposed system, its economic performance is primarily influenced by the fuel used in the reference system, whether natural gas or biomass. In the case of the NG scenario, the proposed system achieves a simple payback (SPB) of approximately 19 years, the most favorable among the scenarios considered. However, this might not be economically viable in real-world applications unless supported by incentive policies like capital investment incentives or feed-in tariffs linked to renewable energy production and utilization.

Future developments in this study will encompass exploring system performance across diverse user profiles and locations, varying energy pricing structures, and incentive policies to identify general conditions for system application. Additionally, a comprehensive sensitivity analysis and rigorous optimization will be conducted to understand how design and economic parameters impact performance. Novel approaches to economic analysis and control strategy will be considered as well.

Funding: This research received no external funding.

Data Availability Statement: Data are contained within the article.

Acknowledgments: The author acknowledges the use of the infrastructure of the Center of Energy, AGH University of Krakow, in Cracow. The author acknowledges the funding program "Pakiet Habilitacyjny" of IDUB AGH University of Krakow.

Conflicts of Interest: The author declares no conflict of interest.

References

1. Lund, H. Renewable energy strategies for sustainable development. *Energy* **2007**, *32*, 912–919. [CrossRef]
2. Jacobsson, S.; Bergek, A. Transforming the energy sector: The evolution of technological systems in renewable energy technology. *Ind. Corp. Chang.* **2004**, *13*, 815–849. [CrossRef]
3. York, R. Do alternative energy sources displace fossil fuels? *Nat. Clim. Chang.* **2012**, *2*, 441. [CrossRef]
4. Su, W.; Wang, J.; Roh, J. Stochastic energy scheduling in microgrids with intermittent renewable energy resources. *IEEE Trans. Smart Grid* **2014**, *5*, 1876–1883. [CrossRef]
5. Twidell, J.; Weir, T. *Renewable Energy Resources*, 3rd ed.; Routledge: Abingdon, UK, 2015.
6. Deshmukh, M.; Deshmukh, S. Modeling of hybrid renewable energy systems. *Renew. Sustain. Energy Rev.* **2008**, *12*, 235–249. [CrossRef]
7. Willis, H.L. *Distributed Power Generation: Planning and Evaluation*, 1st ed.; CRC Press: Boca Raton, FL, USA, 2018.
8. Uddin, M.; Mo, H.; Dong, D.; Elsawah, S.; Zhu, J.; Guerrero, J.M. Microgrids: A review, outstanding issues and future trends. *Energy Strategy Rev.* **2023**, *49*, 101127. [CrossRef]
9. Jung, J.; Villaran, M. Optimal planning and design of hybrid renewable energy systems for microgrids. *Renew. Sustain. Energy Rev.* **2017**, *75*, 180–191. [CrossRef]
10. Qing, K.; Du, Y.; Huang, Q.; Duan, C.; Hu, W. Energy scheduling for microgrids with renewable energy sources considering an adjustable convex hull based uncertainty set. *Renew. Energy* **2024**, *220*, 119611. [CrossRef]
11. Wegener, M.; Malmquist, A.; Isalgué, A.; Martin, A. Biomass-fired combined cooling, heating and power for small scale applications—A review. *Renew. Sustain. Energy Rev.* **2018**, *96*, 392–410. [CrossRef]
12. Morrone, P.; Algieri, A.; Castiglione, T.; Perrone, D.; Bova, S. Investigation of Integrated Organic Rankine Cycles and Wind Turbines for Micro-Scale Applications. *Energy Procedia* **2018**, *148*, 986–993. [CrossRef]
13. Balamurugan, P.; Ashok, S.; Jose, T. An optimal hybrid wind-biomass gasifier system for rural areas. *Energy Sources Part A Recovery Util. Environ. Eff.* **2011**, *33*, 823–832. [CrossRef]
14. Miao, C.; Teng, K.; Wang, Y.; Jiang, L. Technoeconomic Analysis on a Hybrid Power System for the UK Household Using Renewable Energy: A Case Study. *Energies* **2020**, *13*, 3231. [CrossRef]
15. Gonzalez, A.; Riba, J.-R.; Esteban, B.; Rius, A. Environmental and cost optimal design of a biomass–Wind–PV electricity generation system. *Renew. Energy* **2018**, *126*, 420–430. [CrossRef]
16. Zheng, Y.; Jenkins, B.M.; Kornbluth, K.; Træholt, C. Optimization under uncertainty of a biomass-integrated renewable energy microgrid with energy storage. *Renew. Energy* **2018**, *123*, 204–217. [CrossRef]
17. Ahmad, J.; Imran, M.; Khalid, A.; Iqbal, W.; Ashraf, S.R.; Adnan, M.; Ali, S.F.; Khokhar, K.S. Techno economic analysis of a wind-photovoltaic-biomass hybrid renewable energy system for rural electrification: A case study of Kallar Kahar. *Energy* **2018**, *148*, 208–234. [CrossRef]
18. agriKomp Polska Sp. z o.o. Available online: https://www.agrikomp.com/pl/ (accessed on 21 September 2023).
19. Zepter, J.M.; Engelhardt, J.; Gabderakhmanova, T.; Marinelli, M. Empirical validation of a biogas plant simulation model and analysis of biogas upgrading potentials. *Energies* **2021**, *14*, 2424. [CrossRef]

20. Klein, S.A.; Beckman, W.A.; Mitchell, J.W.; Duffie, J.A.; Duffie, N.A.; Freeman, T.L.; Mitchell, J.C.; Braun, J.E.; Evans, B.L.; Kummer, J.P.; et al. *Solar Energy Laboratory, TRNSYS. A Transient System Simulation Program*; University of Wisconsin: Madison, WI, USA, 2006.
21. Charvát, P.; Klimeš, L.; Pech, O.; Hejčík, J. Solar air collector with the solar absorber plate containing a PCM—Environmental chamber experiments and computer simulations. *Renew. Energy* **2019**, *143*, 731–740. [CrossRef]
22. Rosato, A.; Ciervo, A.; Ciampi, G.; Sibilio, S. Effects of solar field design on the energy, environmental and economic performance of a solar district heating network serving Italian residential and school buildings. *Renew. Energy* **2019**, *143*, 596–610. [CrossRef]
23. Roselli, C.; Diglio, G.; Sasso, M.; Tariello, F. A novel energy index to assess the impact of a solar PV-based ground source heat pump on the power grid. *Renew. Energy* **2019**, *143*, 488–500. [CrossRef]
24. ENAIR. Available online: https://www.enair.es/descargas/Ficha_Tecnica/Ficha_Tecnica_E70_en.pdf (accessed on 15 September 2019).
25. INVENSOR. Available online: https://invensor.com/ (accessed on 10 September 2020).
26. TEDOM Poland sp. z o.o. Available online: https://www.tedom.com/pl/ (accessed on 21 September 2023).
27. ABB. *Poland—Energy Efficiency Report*; ABB: Zurich, Switzerland, 2011.
28. Regulation of the Polish Minister of Climate and Environment of December 15, 2022 on the Greenhouse Gas Emission Rate for Electricity in 2023. Available online: https://isap.sejm.gov.pl/isap.nsf/DocDetails.xsp?id=WDU20220002671 (accessed on 21 September 2023). (In Polish)
29. National Centre for Emissions Management (KOBiZE). Available online: https://www.kobize.pl/uploads/materialy/materialy_do_pobrania/monitorowanie_raportowanie_weryfikacja_emisji_w_eu_ets/WO_i_WE_do_monitorowania-ETS-2023.pdf (accessed on 21 September 2023). (In Polish)
30. Calise, F.; Figaj, R.; Vanoli, L. Energy and economic analysis of energy savings measures in a swimming pool centre by means of dynamic simulations. *Energies* **2018**, *11*, 2182. [CrossRef]
31. Di Fraia, S.; Figaj, R.D.; Massarotti, N.; Vanoli, L. An integrated system for sewage sludge drying through solar energy and a combined heat and power unit fuelled by biogas. *Energy Convers. Manag.* **2018**, *171*, 587–603. [CrossRef]
32. Calise, F.; Figaj, R.D.; Vanoli, L. Experimental and numerical analyses of a flat plate photovoltaic/thermal solar collector. *Energies* **2017**, *10*, 491. [CrossRef]
33. Calise, F.; Figaj, R.D.; Vanoli, L. A novel polygeneration system integrating photovoltaic/thermal collectors, solar assisted heat pump, adsorption chiller and electrical energy storage: Dynamic and energy-economic analysis. *Energy Convers. Manag.* **2017**, *149*, 798–814. [CrossRef]
34. Figaj, R. Performance assessment of a renewable micro-scale trigeneration system based on biomass steam cycle, wind turbine, photovoltaic field. *Renew. Energy* **2021**, *177*, 193–208. [CrossRef]
35. Polish Energy Regulatory Office. Available online: https://www.ure.gov.pl/pl/urzad/informacje-ogolne/aktualnosci/11555,Prezes-URE-zatwierdzil-taryfy-na-gaz-na-2024-r.html (accessed on 15 December 2023). (In Polish)
36. TAURON. C12a Tariff. Available online: https://www.tauron.pl/dla-firm/prad/taryfa-sprzedawcy/firma-aktywna-c12a (accessed on 21 September 2023).
37. Polskie Sieci Elektroenergetyczne S.A. Available online: https://www.pse.pl/home (accessed on 21 September 2023).
38. Edwards, S.; Beausoleil-Morrison, I.; Laperrière, A. Representative hot water draw profiles at high temporal resolution for simulating the performance of solar thermal systems. *Sol. Energy* **2015**, *111*, 43–52. [CrossRef]
39. TAURON. Available online: https://www.tauron-dystrybucja.pl/ (accessed on 21 September 2023).
40. OZERISE. Institute for Renewable Energy, Poland. 2011. Available online: https://ozerise.pl/en/ (accessed on 21 September 2023).